Available online at www.sciencedirect.com
ScienceDirect
Journal of Power Sources 163 (2006) 403–408
JOURNAL OF POWER SOURCES
www.elsevier.com/locate/jpowsour

Short communication

Performance of Pt–Co/C prepared by the selective deposition of Co on Pt as a cathode in PEMFCs

Sang Joon Seo, Han-Ik Joh, Hyun Tae Kim, Sang Heup Moon *

School of Chemical & Biological Engineering and Institute of Chemical Process, Seoul National University San 56-1, Shillim-dong, Kwanak-ku, Seoul 151-744, Republic of Korea

Received 10 July 2006; received in revised form 16 August 2006; accepted 15 September 2006
Available online 27 October 2006

Abstract

In this study, Co-modified Pt/C catalysts were prepared by chemical vapor deposition (CVD) of Co on Pt/C. The performance of these catalysts as a cathode in proton exchange membrane fuel cells (PEMFCs), evaluated by a half-cell test, was compared with that of catalysts prepared using the conventional impregnation (IMP) method. The activity of the catalysts for oxygen reduction reaction (ORR) changed showing a maximum with the amounts of added Co and temperatures used for annealing the catalysts.

The amount of Co needed to produce the maximum activity was smaller for the catalysts prepared by CVD ($(Co/Pt)_{CVD} = 0.2$) than those prepared using the IMP method ($(Co/Pt)_{IMP} = 1.0$). Furthermore, the maximum activity of the catalysts prepared by CVD was 1.5 times higher than for the catalysts prepared by IMP.

The ORR activity of the IMP catalyst was degraded by 65% after the corrosion test for 6000 s, which was largely attributed to Co dissolution in the acidic solution, whereas the CVD catalyst showed only 36% degradation. The higher corrosion resistance of the CVD catalyst was attributed to the more intimate Co interactions with the Pt surface than in the catalyst produced using the IMP method.

Keywords: Proton exchange membrane fuel cells; Platinum–cobalt alloy; Chemical vapor deposition; Half-cell test; Oxygen reduction reaction

1. Introduction

Catalysts for proton exchange membrane fuel cells (PEMFCs) are generally evaluated by their activity as a reduction electrode (cathode). This is because the oxygen reduction reaction (ORR) on the electrode has a significant effect on the fuel cell performance [1–8]. There have been many studies on Pt alloy catalysts, which show improved activity and stability in the ORR compared with Pt-only catalysts. Jalan and Taylor [2] attributed the improved performance of Pt alloys as an electrode in phosphoric acid fuel cells (PAFCs) to the shortening of the Pt–Pt interatomic distance induced by alloying. The same phenomenon was reported by Mukerjee and Srinivasan [3]. Watanabe et al. [4] examined well-defined Pt–Co alloys in PAFCs, and reported that alloys with a disordered structure have a higher catalytic activity that is maintained for a longer period than those with an ordered structure. On the other hand, Toda et al. [5] suggested that an increase in the extent of 5d vacancies on the Pt surface, which was induced by the addition of transition metals to the catalyst, led to increased O_2 adsorption and a weakening of the O–O bonds on the surface, resulting in an increased ORR rate. This view was recently supported by Paulus et al. [6] who reported that an oxide layer formed on the Pt surface was easier to reduce, as observed by voltammogram, and consequently the ORR activity was increased for the Pt alloy catalysts.

Another concern in the development of Pt alloy catalysts in fuel cells is the dissolution of the added promoter components in the acidic matrix of the cells, which eventually degrades the activity of the alloy catalysts [9–18]. Pourbaix diagrams [10] indicate that most transition metals, including Co, Cr, Fe, Ni and Cu, are readily soluble in an acidic electrolyte under PEMFC operation conditions. Each metal cation resulting from dissolution can easily exchange with a proton of the perfluoro-sulfonic acid (PFSA) membrane/ionomer [11–13]. Similar results were recently observed by Yu et al. [14] for Pt–Co

* Corresponding author. Tel.: +82 2 880 7409; fax: +82 2 880 1560.
E-mail address: shmoon@surf.snu.ac.kr (S.H. Moon).

0378-7753/$ – see front matter © 2006 Elsevier B.V. All rights reserved.
doi:10.1016/j.jpowsour.2006.09.008

alloys. Colón-Mercado et al. [15,16] monitored the corrosion of metal components and changes in the Pt surface area for Pt and Pt alloy catalysts using an accelerated durability test (ADT). Mukerjee and Srinivasan [17] suggested that the alloy needs to be pre-leached prior to use as a PEMFC electrode in order to minimize contamination of the membrane electrode assembly (MEA) during operation.

Impregnation, which is a general method for preparing the catalyst, involves the promoter component being deposited onto a carbon support as well as on Pt. Hence, the performance of the Pt alloy catalysts prepared by this method does not always vary in proportion to the amount of promoter added. In addition, the catalyst performance is affected by many parameters, such as the Pt particle size, the stoichiometric composition of the Pt alloy, and the degree of alloying. Accordingly, a systematic study is needed to determine a suitable methodology for preparing catalysts in a manner that their properties are precisely controlled.

This study attempted to enhance the performance and stability of PtCo/C for use as a cathode in PEMFCs by preparing the catalyst using a chemical vapor deposition (CVD) method, which allows the selective deposition of Co on the Pt surface as well as the control of the amounts of Co introduced to the surface. The electrocatalytic activity of the prepared catalysts was investigated with regard to the Co loading and the heat-treatment temperatures.

2. Experiments

2.1. Preparation of PtCo/C catalysts

Co was deposited on the surface of a 10 wt% Pt/C catalyst (Johnson Matthey Co., 120 $m^2\,g^{-1}$ Pt) using an atmospheric CVD apparatus (as shown in Fig. 1). $CoCp(CO)_2$ (Dicarbonylcyclopentadienyl cobalt, Aldrich), which is a red liquid with a vapor pressure of 0.5 Torr at room temperature [19], was used as the Co precursor in the CVD process.

The $CoCp(CO)_2$ vapor obtained at room temperature was introduced into the reactor containing the pre-reduced Pt/C catalyst in a flowing hydrogen stream diluted with nitrogen ($H_2/N_2 = 1$) for different periods. The catalyst containing the adsorbed Co precursor was then heated to 300 °C for 1 h in a flowing hydrogen–nitrogen stream in order for the Co precursor to be decomposed on the catalyst surface. The chemical species in the exit stream of the treatment chamber were monitored by FT-IR spectroscopy (Jasco, FT/IR-300E), and the quantity of the individual elements contained in the sample catalysts were analyzed by inductively coupled plasma-atomic emission spectrometry (ICP-AES: Shimadzu, ICPS-1000IV). After Co deposition, the catalyst was treated in a flowing hydrogen–nitrogen stream ($H_2/N_2 = 1/5$) at temperatures up to 800 °C for 1 h in order to allow the added Co form a PtCo alloy. The catalyst prepared using the above procedure is designated as PtCo(C)/C in this paper. A reference PtCo/C catalyst, designated as PtCo(I)/C, was prepared by impregnating 10 wt% Pt/C (Johnson Matthey Co.) with $CoCl_2{\cdot}6H_2O$ (Cobalt(II) chloride hexahydrate, Aldrich), followed by heat-treatment under the same conditions described above.

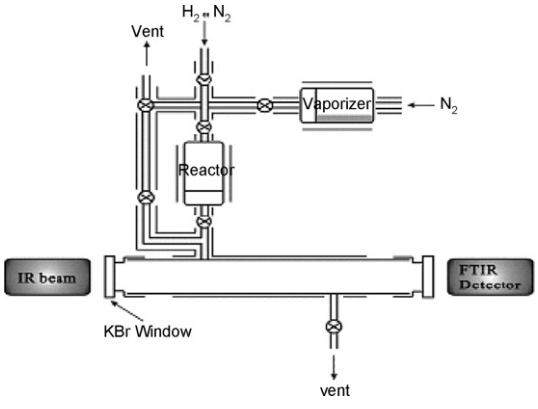

Fig. 1. Schematic diagram of an in situ gas IR cell.

2.2. Activity and stability

The electrochemical activity of the electrode prepared using the Co-modified Pt/C catalyst was tested in a half-cell under the condition of PEMFC operation. The sample catalyst was mixed with a slurry containing isopropyl alcohol and 30 wt% PTFE (polytetrafluoroethylene, Aldrich), the slurry containing the catalyst was pressed onto carbon paper (E-TEK), which was thermally treated at 350 °C for 15 min in an inert gas before its final conversion to an electrode [20,21]. The Pt loading was approximately 2 $mg_{Pt}\,cm^{-2}$, which was higher than one for the state-of-the-art cathode of PEMFC, ca. 0.4 $mg_{Pt}\,cm^{-2}$, because the active area of the electrode for the half-cell tests in this study was very small, 0.78 cm^2. That is, the high Pt loading was used such that the amounts of Co dissolved in electrolyte, particularly from PtCo (CVD), could be quantitatively analyzed by ICP-AES.

The performance of the prepared electrode was determined using a half-cell test. This test was carried out using pure oxygen dissolved in 1 M H_2SO_4 at 60 °C and the cell potential was controlled with a potentiostat (EG&G, M263) [22–24]. The maximum current density was obtained within a few hours. The mass activity, which is defined as the current per unit mass of platinum contained in the electrode, was determined at 0.9 V, using a reversible hydrogen electrode (RHE) as a reference. The stability of the Co-modified Pt/C catalyst was examined by measuring the amount of the catalyst components dissolved in sulfuric acid after an extended period. The dissolved metal ions were analyzed by ICP-AES.

2.3. XRD, TEM and EDS

The average size of the Pt particles in the catalysts was estimated by X-ray diffraction (XRD: Rigaku, 12kw-XRD) using Cu Kα 1.5405 Å radiation. The XRD peaks were assigned based on the database of the Joint Committee on Powder Diffraction Standards (JCPDS), and the lattice parameter (a) was determined for Pt(1 1 1) [25].

Transmission electron microscopy (TEM: JEOL, JEM 3000F) was used to observe the particle sizes directly for

each sample. The chemical compositions of the equivalent-sized alloy particles from the same regions were analyzed by energy-dispersive X-ray spectroscopy (EDS: Oxford, QX-2000) attached to the TEM/STEM. The spot size of the probe (<1.4 nm) was sufficiently small enough to detect the signal from a single particle.

3. Results and discussion

3.1. Selective decomposition of $CoCp(CO)_2$ on Pt

Fig. 2 shows the FT-IR spectra of the gaseous streams at the exit of the reactor, which were obtained after the $CoCp(CO)_2$ vapor had been introduced into the reactor for a pre-determined period and subsequently flushed with an H_2–N_2 mixture. The spectrum for "bypass" in the figure represents the case when the $CoCp(CO)_2$ stream bypassed the reactor, and should be the same as for pure $CoCp(CO)_2$ [26,27].

When the reactor contained the carbon support, the spectrum was similar to that in the bypass case, except for a slight decrease in the overall peak intensity, which indicated that $CoCp(CO)_2$ had not decomposed on the carbon. On the other hand, when the reactor contained Pt/C, the intensity of the $\sqrt{}$(C–O) peaks observed at approximately 2000 cm^{-1} was significantly lower,

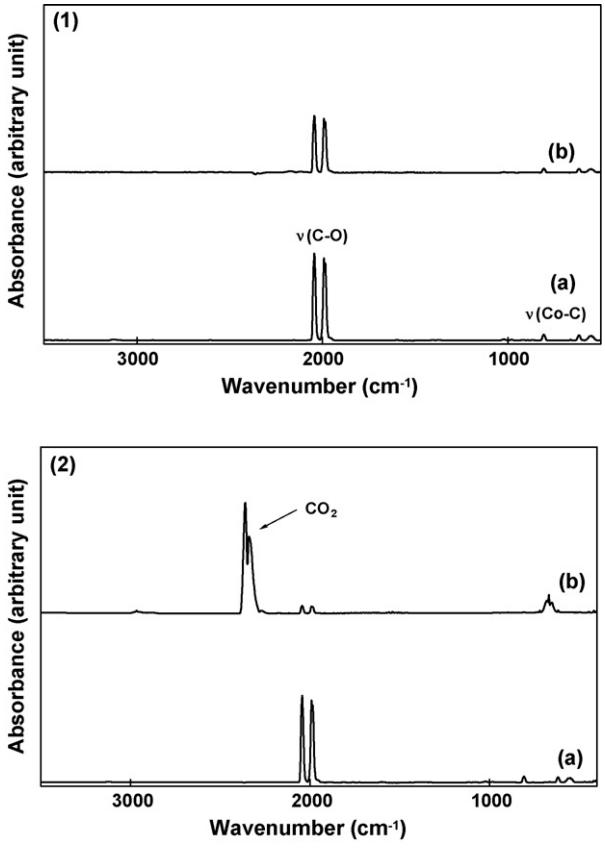

Fig. 2. (1). FT-IR spectra of gas streams at the exit of a reactor containing carbon. Feed = $CoCp(CO)_2$; room temperature; (a) feed bypasses the reactor; (b) feed flows through the reactor for 5 min. (2) FT-IR spectra of gas streams at the exit of a reactor containing Pt/C. Feed = $CoCp(CO)_2$; room temperature; (a) feed bypasses the reactor; (b) feed flows through the reactor for 5 min.

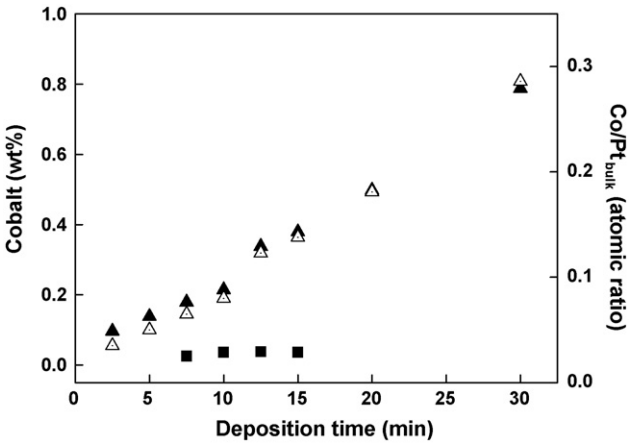

Fig. 3. The amounts of Co deposited on carbon (■) or Pt/C (▲), and the Co/Pt_{bulk} ratio (△) in Pt/C. Co was deposited on the sample by flowing a mixture of H_2 and $CoCp(CO)_2$ through the reactor at room temperature, followed by annealing the sample in H_2/N_2 = 1/1 atmosphere at 300 °C for 1 h.

and a new peak was observed near 2300 cm^{-1}, which was assigned to CO_2. The CO_2, which is formed by a reaction between the CO ligands of $CoCp(CO)_2$ and/or between the CO ligand and the surface intermediates in the form of M = CHOH [28], indicates that the Co precursor decomposed on Pt/C. The Co–Cp bond is less stable than the bonds in the Cp ring itself. Therefore, Co-containing species are likely to be decomposed to metallic Co after the post-treatment in H_2 at 300 °C for 1 h due to dissociation of the Co–Cp bond, [19,29]. The amounts of the Co species remaining on either Pt/C or carbon after the above steps were measured using ICP-AES, and the results are shown in Fig. 3. The amount of Co deposited on Pt/C ranged from 0.1 to 0.8 wt% and increased with increasing deposition time. On the other hand, there was very small amount of Co on carbon even after 15 min deposition. This means that Co deposits selectively on Pt.

3.2. Activity of PtCo/C

Fig. 4 shows the mass activity of the sample catalysts, PtCo(I)/C and PtCo(C)/C. The mass initially increased with increasing Co/Pt atomic ratio but eventually decreased at the ratios higher than an optimum value. This trend is the same as that reported in a previous study [5]. The maximum activity of PtCo(C)/C was obtained at Co/Pt = 0.2, which is approximately 3.9 times higher than that of PtCo(I)/C obtained at a Co/Pt ratio of 0.5. The activity of the alloy catalysts is strongly affected by their annealing temperature [30–32]. Therefore, this study examined the changes in the activity of the above catalysts as a function of the annealing temperature. Fig. 5 shows that the maximum activity of PtCo(C)/C, 9.9*A* g^{-1} pt, is higher and was obtained at a lower annealing temperature, 600 °C, than that of PtCo(I)/C.

These results suggest that there is more surface modification of the Pt surface in the PtCo(C)/C catalyst by the deposited Co than in the PtCo(I)/C catalyst. In order to further examine this phenomenon, the changes in the Pt lattice constant and the aver-

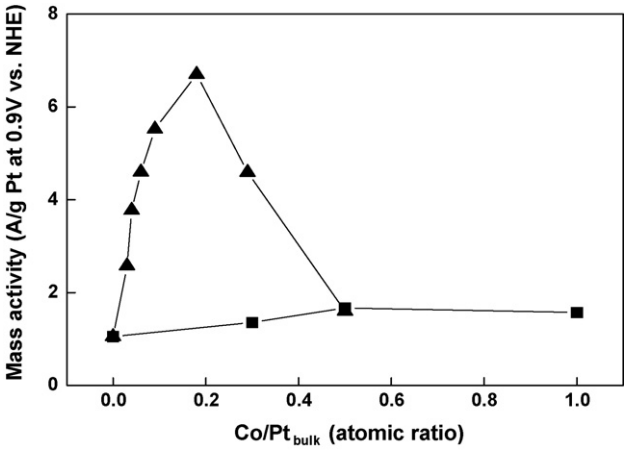

Fig. 4. Changes in the mass activities of PtCo catalysts with the Co/Pt atomic ratio. All catalysts were annealed in H_2/N_2 = 1/1 atmosphere at 300 °C for 1 h. The activity test for oxygen reduction was conducted at 0.9 V vs. NHE in 1 M H_2SO_4 at 60 °C for 4000 s. (▲) PtCo(C)/C; (■) PtCo(I)/C.

age Pt particle size of the catalysts estimated from the XRD patterns were monitored as a function of the annealing temperature. Fig. 6 shows that the lattice constant decreased initially with increasing annealing temperature showing a minimum at approximately 600 °C but eventually increased thereafter. The decrease in the lattice-constant was greater for the catalysts containing a larger Co loading. Unlike the case of the lattice constant, the Pt particle size was relatively unaffected by the annealing temperature up to 600 °C regardless of the catalyst types and compositions but increased significantly at temperatures higher than 600 °C.

According to Fuller et al. [33], the lattice constant of an alloy formed between Pt and a common promoter, e.g. Co or Cr, is lower than that of Pt due to differences in the atomic radii. For example, the atomic radius of Co is 0.125 nm and that Pt is 0.139 nm.

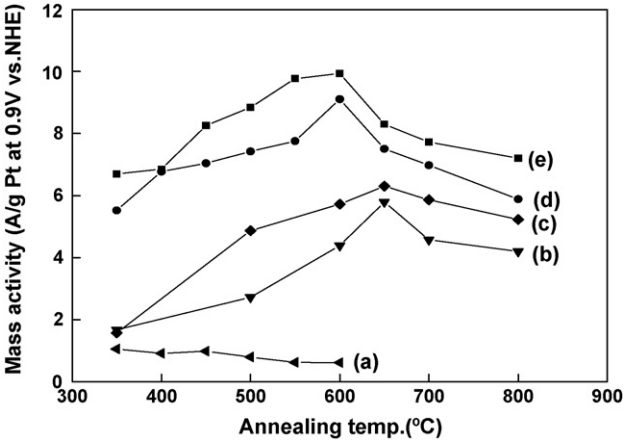

Fig. 5. Changes in the mass activities of PtCo catalysts with the heat-treatment temperature. All catalysts were annealed in H_2/N_2 = 1/5 atmosphere at different temperatures for 1 h. The activity test for oxygen reduction was conducted at 0.9 V vs. NHE in 1 M H_2SO_4 at 60 °C for 4000 s. (a) Pt alone; (b) PtCo(I)/C, Co/Pt = 0.5; (c) PtCo(I)/C, Co/Pt = 1; (d) PtCo(C)/C, Co/Pt = 0.1; (e) PtCo(C)/C, Co/Pt = 0.2.

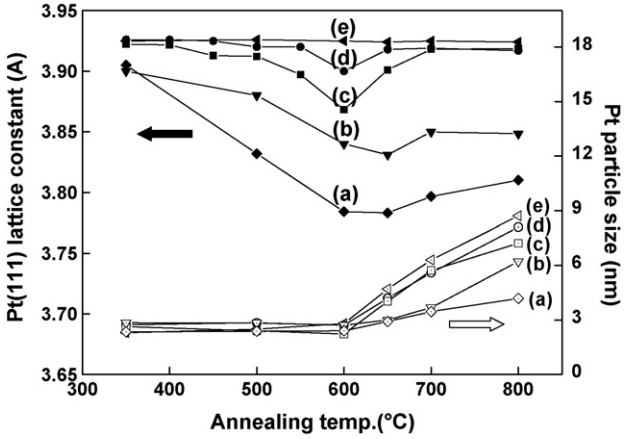

Fig. 6. Changes in the lattice constant (solid) and the particle size (hollow) of PtCo catalysts with the Co/Pt atomic ratio. Lattice constants of Pt were estimated from the XRD peaks of Pt(1 1 1). (a) PtCo(I)/C, Co/Pt = 1; (b) PtCo(I)/C, Co/Pt = 0.5; (c) PtCo(C)/C, Co/Pt = 0.2; (d) PtCo(C)/C, Co/Pt = 0.1; (e) Pt alone.

Watanabe et al. [4] suggested that the thermodynamic stability of the ordered structure of PtCo alloy decreases with increasing annealing temperature above 650 °C, which might lower the intermetallic interaction between Co and Pt. Fig. 6 suggests that the reduction in the lattice constant at temperatures <600 °C was due to the formation of a Pt–Co alloy rather than to changes in the Pt particle size. On the other hand, the lattice constant increases with increasing temperature above 600 °C due to the disordering of the alloy structure, as suggested by Watanabe [4]. Therefore, the activity of PtCo alloy catalysts, as shown in Fig. 5, is closely related to structural changes in the PtCo alloy according to the Co content and annealing temperatures.

3.3. Deactivation of catalysts

Fig. 7 shows the extent of activity degradation for the two catalysts prepared by the impregnation and CVD methods, i.e. PtCo10(I)650 (Co/Pt = 1, annealed at 650 °C) and

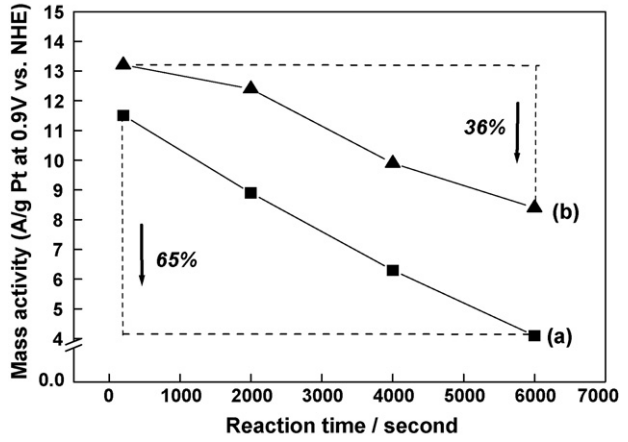

Fig. 7. Changes in the mass activities of PtCo catalysts with the reaction time. All catalysts were annealed in H_2/N_2 = 1/5 atmosphere at different temperatures for 1 h. The activity test for oxygen reduction was conducted at 0.9 V vs. NHE in 1 M H_2SO_4 at 60 °C. (a) PtCo10(I)650:PtCo(I)/C, Co/Pt = 1, annealed at 650 °C; (b) PtCo02(C)600:PtCo(C)/C, Co/Pt = 0.2, annealed at 600 °C.

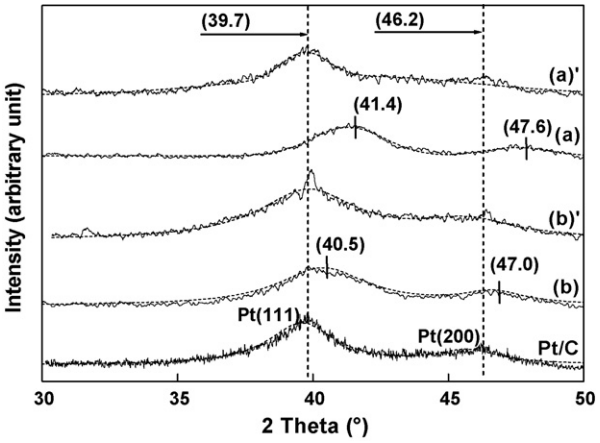

Fig. 8. XRD patterns of PtCo catalysts before and after activity test. The activity test for oxygen reduction was conducted at 0.9 V vs. NHE in 1 M H_2SO_4 at 60 °C for 6000 s. (a) and (a)′ are before and after the test of PtCo10(I)650 (PtCo(I)/C, Co/Pt = 1, annealed at 650 °C), respectively, and (b)′ are before and after the test of PtCo02(C)600 (PtCo(C)/C, Co/Pt = 0.2, annealed at 600 °C), respectively.

PtCo02(C)600 (Co/Pt = 0.2, annealed at 600 °C), as a function of the reaction time. The two catalysts were selected because they showed the maximum initial activity among the catalysts of the specific types (Fig. 5). The mass activity of PtCo10(I)650 decreased by approximately 65% (from 11.5 A g_{Pt}^{-1} to 4.1 A g_{Pt}^{-1}) after a reaction for 6000 s. In contrast, the mass activity of PtCo02(C)600 decreased by approximately 36% (from 13.2 A g_{Pt}^{-1} to 8.4 A g_{Pt}^{-1}).

Fig. 8 shows the XRD patterns of the catalysts before and after the reaction test for 6000 s. In the case of the unmodified Pt/C, the peaks associated with the Pt(1 1 1) and (2 0 0) planes were observed at 39.7° and 46.2°, respectively. However, these peaks were observed at higher angles in the case of the PtCo catalysts but eventually shifted to the same positions as for Pt/C after the reaction test. The initial shifts in the peak positions to higher angles for the PtCo catalysts indicate a decrease in the lattice constant in the presence of Co, which indicates the formation of a PtCo alloy. The extent of alloy formation was smaller for PtCo02(C)600 than for PtCo10(I)650 because the former contained a smaller amount of Co. The final return of the peak positions to those of Pt/C after the test suggests that the alloy effect was almost eliminated due to Co dissolution in the acidic solution, as is frequently observed in the practical operations of the PEMFC [4,34].

Table 1 shows the relative amounts Co dissolved from the sample catalysts before and after the test reaction. The relative amounts of dissolved Co were 0.60 and 0.63 for PtCo05(I)650 and PtCo10(I)650, respectively, while the amount was only 0.30

Table 1
The amounts of Co dissolved in sulfuric acid solution during activity test

Sample	Initial, Co/Pt (A)	After test, Co/Pt (B)	Co dissolution (A − B)/A
PtCo05(I)650	0.5	0.20	0.60
PtCo10(I)650	1	0.37	0.63
PtCo02(C)600	0.2	0.14	0.30

Tested at 0.9 V vs. NHE and 60 °C in 1 M H_2SO_4 for 6000 s.

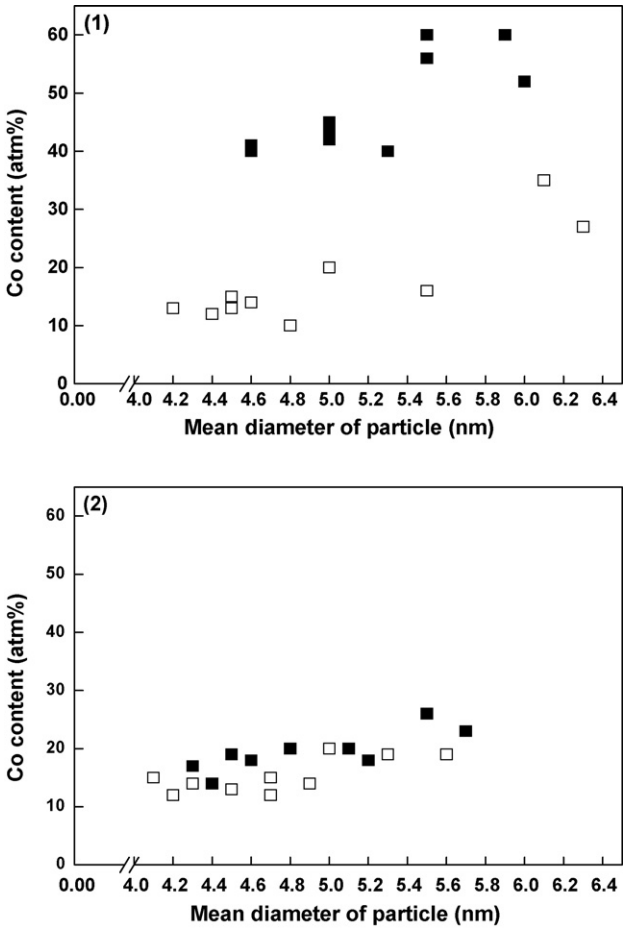

Fig. 9. (1) The correlation between the Co content (measured by EDS) and the particle size (measured by TEM) for PtCo10(I)650 before (■) and after (□) the activity test. The test was conducted for oxygen reduction at 0.9 V vs. NHE in 1 M H_2SO_4 at 60 °C for 6000 s. (2) The correlation between the Co content (EDS) and the particle size (TEM) for PtCo02(C)600 before (■) and after (□) the activity test. The test was conducted for oxygen reduction at 0.9 V vs. NHE in 1 M H_2SO_4 at 60 °C for 6000 s.

for PtCo02(C)600. It should be noted that the extent of Co dissolution was similar for the two PtCo(I)/C catalysts even though their initial Co content was quite different. Therefore, Co was dissolved from PtCo(C)/C to a lesser extent than from PtCo(I)/C.

EDS was used to quantify the Co contained in the individual particles before and after the reaction tests in order to determine the extent of Co dissolution from the catalysts. The results shown in Fig. 9 need to be analyzed in three aspects. The first aspect is that the Co content of the individual particles was higher in the larger particles, which suggests that Co affects the particle size by forming aggregates of Co and Pt. The above result is indirect evidence showing that the added Co interacts with Pt particles. The second aspect is that the Co contents in the particles of the same sizes before the reaction test were significantly larger for the PtCo10(I)650 catalyst than for the PtCo02(C)600. This result can be obtained when relatively large amounts of Co are associated with the Pt particles or are dispersed as independent particles on the support in PtCo(I)650 compared with the case of PtCo02(C)600. The third aspect is that, after the reaction test, the Co content of the particles were decreased significantly

for PtCo10(I)650 but was only decreased to a small extent for PtCo02(C)600. Overall, in PtCo(C)/C, the added Co interacts closely with Pt and is stabilized by alloy formation while, with PtCo(I)/C, the Co species are loosely associated with Pt and are more prone to dissolution in an acidic solution than the PtCo(C)/C catalyst.

There is a discrepancy in the relative amounts of dissolved Co shown Table 1 and Fig. 9, which were obtained in the dissolution tests carried out under the identical conditions. The discrepancy was obtained because, in the case of Fig. 9, the Co contents were obtained by analyzing the individual particles of the same sizes. However, the Co content should be integrated over the whole range of particle sizes, as was done for the analysis in Table 1.

4. Conclusion

Pt/C catalysts promoted by Co deposited selectively on the Pt surface by CVD showed higher ORR activities at a smaller Co content than those containing Co added by impregnation. The rate of degradation in the catalytic activity for ORR of the PtCo(I)/C catalyst after the test reaction for 6000 s was approximately double that of the PtCo(C)/C catalysts. The amount of Co dissolved in the acidic electrolyte after the reaction for 6000 s were also smaller in the PtCo(C)/C catalyst (approximately 50%) than in the PtCo(I)/C catalyst.

Consequently, a PtCo alloy was formed more efficiently in the catalyst containing Co deposited by CVD as a result of the strong interaction between the Pt and Co, which promoted the activity and acid-resistance of the catalyst.

Acknowledgements

This work was supported by the Brain Korea 21 project, the Engineering Research Institute of Seoul National University, the Core Technology Development Program for Fuel Cell of Ministry of Commerce, Industry and Energy, and National Research Laboratory Program of Ministry of Science and Technology, Korea.

References

[1] N.M. Markovic, B.N. Grgur, P.N. Ross, J. Phys. Chem. B. 101 (1997) 5405.
[2] V. Jalan, E.J. Talyor, J. Electrochem. Soc. 130 (1983) 2299.
[3] S. Mukerjee, S. Srinivasan, J. Electroanal. Chem. 357 (1993) 201.
[4] M. Watanabe, K. Tsurumi, T. Mizukami, T. Nakamura, P. Stonehart, J. Electrochem. Soc. 141 (1994) 2659.
[5] T. Toda, H. Igarashi, H. Uchida, M. Watanabe, J. Electrochem. Soc. 146 (1999) 3750.
[6] U.A. Paulus, A. Wokaun, G.G. Scherer, T.J. Schmidt, V. Stamenkovic, N.M. Markovic, P.N. Ross, Elecrochimica Acta 47 (2002) 3787.
[7] S.K. Park, E.A. Cho, I.H. Oh, Korean J. Chem. Eng. 22 (6) (2005) 877.
[8] V. Stamenkovic, T.J. Schmidt, P.N. Ross, N.M. Markovic, J. Phys. Chem. B 106 (2002) 11970.
[9] T.R. Ralph, M.P. Hogarth, Platinum Met. Rev. 46 (2002) 3.
[10] M. Pourbaix, Altas of Electrochemical Equilibrium in Aqueous Solutions, Pergamon Press, New York, 1966.
[11] T. Okada, Y. Ayato, M. Yuasa, I. Sekine, J. Phys. Chem. B 103 (1999) 3315.
[12] T. Okada, Handbook of Fuel Cells—Fundamental, Technology, and Applications, vol. 3, 2003, p. 647.
[13] T. Okada, Y. Ayato, H. Satou, M. Yuasa, I. Sekine, J. Phys. Chem. B 105 (2001) 6980.
[14] P. Yu, M. Pemberton, P. Plasse, J. Power Sources 144 (2005) 11.
[15] H.R. Colón-Mercado, H. Kim, B.N. Popov, Electrochem. Commun. 6 (2004) 795.
[16] H.R. Colón-Mercado, H. Kim, B.N. Popov, J. Power Sources 155 (2) (2006) 253.
[17] S. Mukerjee, S. Srinivasan, Handbook of Fuel Cells—Fundamental, Technology, and Applications, vol. 2, 2003, p. 502.
[18] D.A. Landsman, F.J. Luczak, Handbook of Fuel Cells—Fundamental, Technology, and Applications, vol. 4, 2003, p. 811.
[19] G.J.M. Dormans, G.J.B. Meekes, E.G.J. Staring, J. Cryst. Growth 114 (1991) 364.
[20] M. Watanabe, M. Tomokawa, S. Motoo, J. Electroanal. Chem. 195 (1985) 81.
[21] N. Giordano, E. Passalacqua, V. Alderucci, P. Staiti, L. Pino, H. Mirzaian, E.J. Taylor, G. Wilemski, Electrochim. Acta 36 (1991) 1049.
[22] E. Gugliemotti, J. Mol. Catal. 13 (1981) 207.
[23] K. Kinoshita, J. Lundquist, P. Stonehart, J. Catal. 31 (1973) 325.
[24] M. Peuckert, T. Yoneda, M. Boudart, J. Electrochem. Soc. 133 (1986) 944.
[25] J.T. Hwang, J.S. Chung, Electrochim. Acta 38 (1993) 2715.
[26] C. Ficket, P. Günther, P. Scholz, D. Gernet, R. Pikl, W. Kiefer, Inorg. Chim. Acta 251 (1996) 157.
[27] G.M. Hansford, P.B. Davies, J. Gang, D.K. Russell, Spectrochim. Acta 53 (1997) 1755.
[28] R.P. Eischens, W.A. Pliskin, Adv. Catal. X (1958) 1.
[29] G.J.M. Dormans, J. Cryst. Growth 108 (1991) 806.
[30] L.J. Bregoli, Electrochim. Acta 23 (1978) 489.
[31] M. Watanabe, H. Sei, P. Stonehart, J. Electroanal. Chem. 216 (1989) 375.
[32] P. Stonehart, Phys. Chem. 94 (1990) 913.
[33] T.F. Fuller, F.J. Luczak, D.J. Wheeler, J. Electrochem. Soc. 142 (1995) 1752.
[34] H.A. Gasteiger, S.S. Kocha, B.S. Sompalli, F.T. Wagner, Appl. Catal. B 56 (2005) 9.